

Efficient adiabatic preparation of tensor network states

Zhi-Yuan Wei , Daniel Malz , and J. Ignacio Cirac *Max-Planck-Institut für Quantenoptik, Hans-Kopfermann-Straße 1, D-85748 Garching, Germany
and Munich Center for Quantum Science and Technology (MCQST), Schellingstraße 4, D-80799 München, Germany* (Received 26 September 2022; revised 19 January 2023; accepted 18 April 2023; published 22 May 2023)

We propose and study a specific adiabatic path to prepare those tensor network states that are unique ground states of few-body parent Hamiltonians in finite lattices, which include normal tensor network states, as well as other relevant nonnormal states. This path guarantees a gap for finite systems and allows for efficient numerical simulation. In one dimension, we numerically investigate the preparation of a family of states with varying correlation lengths and the one-dimensional Affleck-Kennedy-Lieb-Tasaki (AKLT) state and show that adiabatic preparation can be much faster than standard methods based on sequential preparation. We also apply the method to the two-dimensional AKLT state on the hexagonal lattice, for which no method based on sequential preparation is known, and show that it can be prepared very efficiently for relatively large lattices.

DOI: [10.1103/PhysRevResearch.5.L022037](https://doi.org/10.1103/PhysRevResearch.5.L022037)

Introduction. Matrix product states (MPS) [1,2] and more generally projected entangled-pair states (PEPS) [3] capture the physical properties of systems obeying the entanglement area law [4]. PEPS contain a rich set of many-body states [5] such as the cluster state [6], toric codes [7], Greenberger-Horne-Zeilinger (GHZ) state [8], and W state [9] in quantum information, and the Affleck-Kennedy-Lieb-Tasaki (AKLT) states [10,11], valence-bond states [12], and string net states [13] in condensed matter physics. There is thus increasing interest in finding ways of preparing them in quantum computers or quantum simulators, either for quantum information applications like computing [14], metrology [15], communication, and networking [16], or as variational states for the study of many-body quantum systems [17].

MPS are most naturally prepared sequentially [18], which requires a time that scales linearly in the number of sites N . In higher dimensions, for PEPS, this is not possible in general [19]. However, certain subclasses of PEPS can be generated sequentially in linear time [20–23]. Sequential preparation has been used in various platforms to experimentally prepare MPS and PEPS [24–27].

Besides quantum circuits, adiabatic algorithms are also widely used to prepare many-body states on quantum devices [28]. By smoothly tuning the Hamiltonians along a gapped path that connects a trivial state to the target state, quasiadiabatic evolution for a time T produces a state very close to the target state. Adiabatic algorithms have been proposed to prepare PEPS [29–32], and, in particular, Ref. [31] proved that it is possible to prepare a generic family of them, so-called *normal* PEPS [1,2], in time $T = O(\text{polylog}N)$ with

a specific method that switches on and off certain Hamiltonian terms adiabatically and provided there exists a gap along the whole path that is lower bounded by a constant. A method to compute such a lower bound based on semidefinite programming has been presented in Ref. [32]. While those methods provide rigorous proofs for the asymptotic limit $N \gg 1$, it is not clear how they perform in practice, in particular for the intermediate sizes available in the near term. For such cases, there is no guarantee that they provide any advantage with respect to sequential methods.

In this paper, we propose a specific adiabatic path to prepare PEPS in any dimension that are unique ground states of local frustration-free Hamiltonians and analyze its performance. Our path guarantees the existence of a gap (for finite systems), and in contrast to Refs. [31,32] yields Hamiltonian with substantially smaller support for preparing the two-dimensional (2D) AKLT state on the hexagonal lattice. Moreover, it extends to certain nonnormal PEPS [33], which allows us to prepare the AKLT states in arbitrary geometries.

Since the ground states along our path are always PEPS, we are able to simulate relatively large systems, which we use to numerically determine the performance of the algorithm. In one dimension (1D), we consider the family of MPS introduced in Ref. [34], which allows us to investigate how the efficiency of the algorithm depends on correlation length. We also consider the paradigmatic 1D AKLT state. We obtain that for system sizes up to $N = 5000$, the preparation can be much more efficient than sequential preparation, with $T \sim \text{polylog}N$ in the regime we study [35]. In 2D, our adiabatic path overcomes several difficulties and allows us to simulate the adiabatic preparation of the 2D AKLT state on the hexagonal lattice up to $N \sim 10 \times 10$. Our results indicate that adiabatic preparation is very efficient also in higher dimensions.

PEPS. PEPS can be built by applying local commuting operators to a product state of maximally entangled pairs in a lattice [3,36]. Let us consider a regular lattice denoted by a

Published by the American Physical Society under the terms of the [Creative Commons Attribution 4.0 International license](https://creativecommons.org/licenses/by/4.0/). Further distribution of this work must maintain attribution to the author(s) and the published article's title, journal citation, and DOI. Open access publication funded by the Max Planck Society.

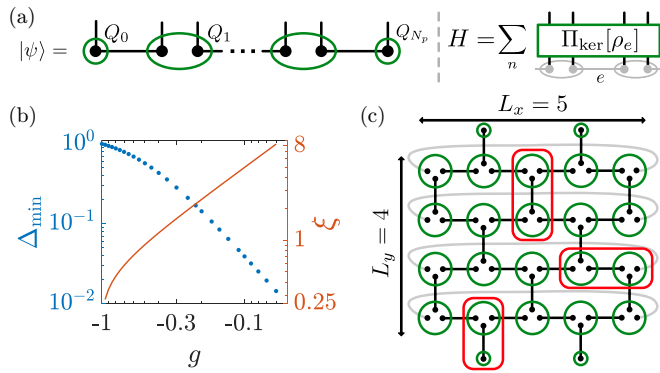


FIG. 1. Adiabatic preparation of MPS and PEPS. (a) In 1D, a MPS $|\psi\rangle$ [Eq. (1)] is constructed by applying a set of operators $\{Q_v\}$ (green circles) on a product of pairs of maximally entangled virtual qudits (the connected dots). $|\psi\rangle$ is the ground state of a local Hamiltonian H [Eq. (3)], which can be taken to be the sum of projectors (green rectangle) onto the kernel of the corresponding reduced density matrices. (b) The minimal gap Δ_{\min} of the adiabatic path [cf. Eq. (6)] (computed with $N = 400$ sites here, but it is size independent [33]) and the correlation length ξ for states in the MPS family [cf. Eq. (4)]. (c) 2D PEPS on the hexagonal lattice. The green circles denote the operators $\{Q_v\}$, and the connected dots denote maximally entangled virtual qudit pairs. Each term of the parent Hamiltonian H acts on neighboring sites (shown as red rectangles). The size of the lattice is $L_x \times L_y$. In our numerics, we focus on the 2D AKLT state on the hexagonal lattice with cylinder boundary conditions (illustrated through gray lines).

graph \mathcal{G} , with edges \mathcal{E} and sites \mathcal{V} . The coordination number of site $v \in \mathcal{V}$ is n_v ; i.e., each site contains n_v virtual qudits. Defining local operators $\{Q_v\}$ that map the D -level virtual qudits on site $v \in \mathcal{V}$ to a d -level physical site, the PEPS is expressed as [see Fig. 1(a) for 1D case and Fig. 1(c) for 2D hexagonal lattice case]

$$|\psi\rangle \propto \bigotimes_{v \in \mathcal{V}} Q_v \bigotimes_{e \in \mathcal{E}} |\Phi^+\rangle_e, \quad (1)$$

with $|\Phi^+\rangle \propto \sum_{\alpha=0}^{D-1} |\alpha\alpha\rangle$. Here D is the bond dimension of the PEPS, and d is the physical dimension. For instance, MPS can be viewed as 1D PEPS with $n_v = 2$ virtual qudits per site [cf. Fig. 1(a)]. The matrix representation of $\{Q_v\}$ in the bulk for MPS then reads

$$Q_v^{\text{1D}} = \sum_{i_v=0}^{d-1} \sum_{\alpha_v, \beta_v=0}^{D-1} A_{[v]_{\alpha_v \beta_v}}^{i_v} |i_v\rangle \langle \alpha_v \beta_v|. \quad (2)$$

The operators on the boundary each act on a single qudit [37]. By blocking neighboring sites, we can enlarge the physical dimension such that $d \geq D^{n_v}$. In this case, without loss of generality, we can apply a polar decomposition to write $\{Q_v\}$ as positive-semidefinite operators with $d = D^{n_v}$, which holds for arbitrary PEPS up to a layer of local isometries [33]. A PEPS is called *injective* if $\{Q_v\}$ are left invertible [1,2]. If the operators obtained after blocking a finite number of sites are invertible, the PEPS is called *normal*.

In this paper, we aim to prepare a large class of PEPS that are unique ground states of local frustration-free Hamiltonians. This includes all normal (and thus all injective)

PEPS [1,2], but also other relevant states like the AKLT states (possibly nonnormal [33,36]), where a much simpler parent Hamiltonian is known [10,11]. In particular, we consider the following parent Hamiltonian [34,38] [cf. Fig. 1(a)]

$$H = \sum_e \Pi_{\ker}[\rho_e], \quad (3)$$

where Π_{\ker} projects on the kernel of ρ_e , which is the reduced density matrix of neighboring sites around the edge $e \in \mathcal{E}$ [39]. Note that $\|\Pi_{\ker}[\rho_e]\| = 1$, and thus the time is unitless in this paper.

The parent Hamiltonian H [Eq. (3)] for injective PEPS has a unique ground state [38], which implies a nonzero gap that may depend on the system size N . Moreover, H for 1D injective MPS is guaranteed to be gapped also in the thermodynamic limit [1]. Finally, H for the AKLT states is equivalent to the known two-body parent Hamiltonian [10,11].

Examples. We study two paradigm examples of PEPS in this paper. The first example is a family of MPS of bond dimension $D = 2$ [34]. In this case the graph \mathcal{G} corresponds to a chain formed by $N = 2N_p$ qubits forming N_p pairs [cf. Fig. 1(a)]. After blocking each neighboring two sites, we arrive at the injective form of the MPS family for $g \neq 0$ (with $d = D^2 = 4$), where the matrices in Eq. (2) are given through

$$\begin{aligned} A_{[v]}^0(g) &= \begin{pmatrix} 0 & g \\ 1 & 0 \end{pmatrix}, & A_{[v]}^1(g) &= \begin{pmatrix} 0 & g \\ 1 & 0 \end{pmatrix}, \\ A_{[v]}^2(g) &= \begin{pmatrix} 0 & 1 \\ 1 & 0 \end{pmatrix}, & A_{[v]}^3(g) &= \begin{pmatrix} 0 & g \\ g & 0 \end{pmatrix}. \end{aligned} \quad (4)$$

The corresponding parent Hamiltonian [Eq. (3)] acts only on nearest neighbors, but with each site containing two qubits.

We will study the preparation of states with $g \in (-1, 0)$, which interpolates between the cluster state ($g = -1$) and the GHZ state ($g = 0$). For $g < 0$, the correlation length ξ of the MPS family can be obtained as [cf. Fig. 1(b)]

$$\xi = \left(\ln \frac{1-g}{1+g} \right)^{-1}. \quad (5)$$

Thus by tuning g , we can explore the effect of correlation length on the performance of the adiabatic algorithm. Note that $g \in (-1, 0)$ already covers all states with $g < 0$, since the tensors $\{A(g)\}$ in Eq. (4) can be mapped to $\{A(1/g)\}$ by a gauge transformation [40].

The other example we consider is the 1D AKLT state of spin $S = 1$ and the 2D AKLT state of spin $S = 3/2$ in the hexagonal lattice [cf. Fig. 1(c)] [10,11]. AKLT states can be formed by first having a product state of singlets consisting of virtual qubits that connect neighboring sites of the lattice, then projecting the virtual qubits at each site v to their symmetric subspace. AKLT states can be written as $D = 2$ PEPS [Eq. (1)], and we promote the virtual qubits into physical ones, such that the operators $\{Q_v\}$ are already positive-semidefinite without blocking [33].

Adiabatic algorithm. We propose an adiabatic path parametrized by s , which connects a product state of maximally entangled pairs $|\psi(0)\rangle \equiv \bigotimes_{e \in \mathcal{E}} |\Phi^+\rangle_e$ [41] to the target PEPS $|\psi(1)\rangle \equiv |\psi\rangle$. We choose the instantaneous ground states $|\psi(s)\rangle$ in this path to be always PEPS of bond dimension

D , with [see Eq. (1)]

$$Q_v(s) = sQ_v + (1-s)\mathbb{1}. \quad (6)$$

For all s , one can construct the parent Hamiltonian $H(s)$ [cf. Eq. (3)] such that $|\psi(s)\rangle$ is its ground state. This path has the following features:

(1) Adiabatic evolution along this path can be classically simulated (approximately), as its instantaneous ground states $|\psi(s)\rangle$ [cf. Eq. (6)] are PEPS of bond dimension D [3].

(2) This path is gapped for finite systems. First, for $s \in [0, 1]$, $\{Q_v(s)\}$ are invertible (since $\{Q_v\}$ are positive semidefinite), and thus the Hamiltonian $H(s)$ along the path has a nonzero gap $\Delta(s) > 0$. For $s = 1$ we also have $\Delta(1) > 0$ since we consider the class of PEPS that are unique ground states of local Hamiltonians [Eq. (3)]. As for finite systems, $\Delta(s)$ is continuous and differentiable in the whole interval $s \in [0, 1]$ and the derivative $d\Delta(s)/ds$ is finite, which immediately implies that $\Delta(s) \geq \Delta_{\min} > 0$ (note that Δ_{\min} may depend on the system size N).

(3) The support of each term in the Hamiltonian $H(s)$ [Eq. (3)] stays the same for all $s \in [0, 1]$, which may simplify the experimental implementation. For example, for preparing AKLT states, $H(s)$ is always two body.

In the following, we study the adiabatic preparation of these examples using our path.

Preparation of the MPS family. First, we computed the minimal gap Δ_{\min} during the adiabatic path [cf. Eq. (6)] for the MPS family [cf. Eq. (4)] in Fig. 1(b). One can see that Δ_{\min} decreases as the correlation length ξ increases, which suggests that the adiabatic algorithm should perform better when the correlation length is smaller.

We classically simulate the quasiadiabatic time evolution of a chain of N qubits for a time T [33], following the path in Eq. (6), where we take the interpolation function $s(t/T)_{1D} \equiv \sin^2[\pi/2 \cdot \sin^2(\pi t/2T)]$ [42].

Assuming that the state we obtained after the evolution is $|\phi(T)\rangle$, its fidelity \mathcal{F} compared to the target state $|\psi(1)\rangle$ is $|\langle\psi(1)|\phi(T)\rangle|^2$. For all fixed $T \geq 0$, we numerically find that \mathcal{F} decays exponentially with system size N [33], which allows us to define an error density $\kappa(T)$ that is independent of system size. Thus, we can write

$$\mathcal{F}(N, T) = \exp[-\kappa(T) \cdot N - c(T)], \quad (7)$$

where $c(T)$ is an error that comes from the boundaries of the system and is independent of N . This indicates that during the adiabatic dynamics, the errors in different regions of the chain change almost uniformly.

The error density $\kappa(T)$ can be obtained by fitting the fidelity of preparing the same state of various system sizes N and a fixed time T using the scaling Eq. (7) [33]. In Fig. 2(a), we show $\kappa(T)$ for the MPS family as a function of T , and it features two regimes. When T is small, the dynamics is not adiabatic, and we see $\kappa(T)$ already starts to decay quickly. When T becomes larger, $\kappa(T)$ enters a regime of almost exponential decay, which we fit with

$$\kappa(T) \approx \kappa_0 \exp(-\gamma T). \quad (8)$$

The decay rate γ decreases with increasing correlation length ξ [see Fig. 2(c)], and the boundary term $|c(T)|$ shows a similar behavior as $\kappa(T)$ [33]. Note that, due to the finite smoothness

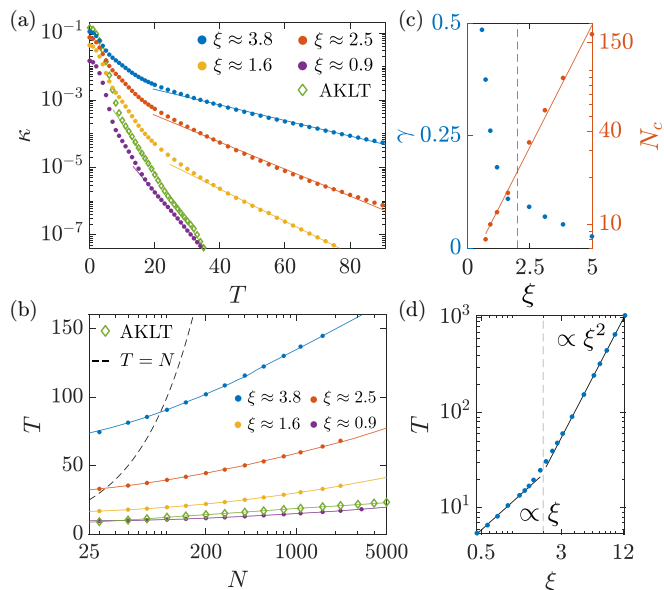


FIG. 2. (a) The error density $\kappa(T)$ [cf. Eq. (7)] as a function of the adiabatic evolution time T , for preparing states in the MPS family with various correlation length ξ as well as the 1D AKLT state. The lines are exponential fits to the data. (b) Time T for preparing the same set of states in panel (a) of size N with fidelity $\mathcal{F} = 0.99$. The dots are obtained by the numerical simulation, while the solid lines are the prediction of Eq. (7). The dashed line denotes the scaling for the sequential method (assuming it takes a time $T = N$). (c) The decay rate γ [cf. Eq. (8)] and the system size N_c where the adiabatic method and sequential method give the same preparation time ($T = N_c$) as a function of the correlation length ξ for the MPS family. The vertical dashed lines in panels (c) and (d) correspond to the size of each lattice site ($\xi = 2$). (d) Time T to prepare states in the MPS family of fixed particle number $N = 100$, as a function of the correlation length ξ .

of the interpolation function $s(t/T)_{1D}$ we use, we expect that $\kappa \sim 1/\text{poly}(T)$ when $T \rightarrow \infty$ [33,43–46]. One can extend the range of the exponential decay by making the interpolation function smoother, however, at the expense of reducing the decay rate γ [33].

In Fig. 2(b), we show the dependence of time T required to prepare the given target state with fidelity $\mathcal{F} = 0.99$ on system size N up to $N \approx 5000$. The results agree well with the simple expression Eq. (7), which lead to $T \sim \text{polylog } N$ in this regime (which is the relevant regime experimentally). We also compare the adiabatic preparation to sequential preparation [18], which we assume takes a time $T = N$ [see Fig. 2(b)]. One sees that the adiabatic algorithm outperforms the sequential preparation method in terms of the preparation time T when the system size N is larger than a threshold value $N_c(\xi)$ [47]. We find numerically that [cf. Fig. 2(c)] N_c almost grows exponentially with ξ , which indicates that when the correlation length is smaller than a fraction of the system size, the adiabatic algorithm prepares the MPS family [cf. Eq. (4)] faster than the sequential method.

Finally, we show the time T to prepare states of system size $N = 100$ as a function of the correlation length ξ in Fig. 2(d). We observe $T \propto \xi$ ($T \propto \xi^2$) when ξ is smaller (larger) than the length of the lattice site, which is $\xi = 2$ since each site

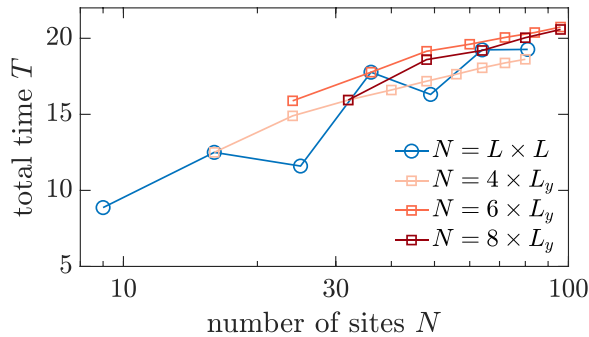


FIG. 3. The evolution time T needed to prepare the 2D AKLT state on the hexagonal lattice with fidelity $\mathcal{F} = 0.99$ for $N = L \times L$ ($L = 3 - 9$) and $N = L_x \times L_y$ with various fixed $L_x = 4, 6, 8$. The lines are visual guides.

contains two qubits. This shows that the size of each lattice site sets another length scale in the system, and one can also see such behavior for the decay rate γ shown Fig. 2(b).

Preparation of AKLT states. Now we study the preparation of the 1D and 2D AKLT states using our adiabatic path. In 1D, it has been proposed to prepare the AKLT state sequentially [18], dissipatively [48], using measurements [49], or by fusing multiple AKLT chains in parallel [48], which has the best known preparation time $T = O(\log^2 N)$. In Figs. 2(a) and 2(b), we show the results for adiabatic preparation of the 1D AKLT state using our adiabatic path. As expected, $T \sim \text{polylog } N$ up to $N = 5000$.

Preparation of the 2D AKLT states are much less explored. For the case of hexagonal lattice, this state have a gapped parent Hamiltonian [50,51], and there is indirect evidence suggesting that this state can be adiabatically prepared with $T = O(N)$ [52]. The general protocol [31,32] predicts the preparation time $T = O(\text{polylog } N)$ when $N \gg 1$, but it faces the following challenges: First, the construction of the parent Hamiltonian there requires the target PEPS to be normal, which does not work for nonnormal PEPS such as the 2D AKLT state on the square lattice [36], or leads to a Hamiltonian for the 2D AKLT state on the hexagonal lattice that acts on large clusters [53], making it difficult to implement in current devices. More importantly, it is difficult to simulate an adiabatic evolution in 2D since the time cost of classical simulation algorithms typically has heavy dependence on the bond dimension of the underlying PEPS [54].

Our adiabatic path overcomes the above problems (partially because we promote the virtual qubits to physical ones [33]). The Hamiltonian [cf. Eq. (3)] along the whole path is two body and gapped (note that each site contain three qubits). Moreover, the instantaneous ground state [cf. Eq. (6)] is always a PEPS of bond dimension $D = 2$ [55].

We classically simulate the preparation of the 2D AKLT state on the hexagonal lattice with cylinder boundary condition, and $N \equiv L_x \times L_y$ sites [cf. Fig. 1(c)] [33] using the interpolation function [cf. Eq. 6] $s(t, T)_{2D} \equiv \sin^2(\pi t/2T)$ [42].

In Fig. 3, we show the preparation time T needed to reach a fidelity $\mathcal{F} = 0.99$ for different system sizes N . In the case of $N = L \times L$, since each hexagon is of size 2×1 [cf. Fig. 1(c)],

for even or odd L the boundary affects T differently. We see that overall T is practically short ($T \approx 10$), and increases only mildly with system size N . We also show T for preparing this state of lattice size $N = L_x \times L$ by fixing different $L_x = 4, 6, 8$, and observe similar behavior. In particular, the lattice geometry does not strongly affect the preparation time T , as it takes a similar T to prepare the state on a 4×20 lattice or 9×9 lattice.

We expect that T will still be practically short when we increase the system size further than that shown in Fig. 3. Moreover, the general nature of the proposed path suggests that this method may be used to efficiently prepare a large variety of (high-dimensional) PEPS. For example, in the Supplemental Material [33], we provide numerical evidence that the 2D AKLT state on the square lattice can be prepared with this method.

Outlook. We have proposed and studied a specific adiabatic path to prepare a large family of MPS and PEPS, which applies to the normal PEPS and other relevant PEPS like the AKLT states.

It is worth checking if the 2D AKLT state of $N \gg 100$ can still be efficiently prepared using quantum devices, and exploring the performance of this adiabatic path to prepare other (potentially nonnormal [36]) PEPS. By studying the gap during the adiabatic path in the thermodynamic limit [32,56], it is possible to probe the asymptotic behavior of the adiabatic algorithm and further improve its performance with adiabatic ramp rate that adapts to the magnitude of the gap. Moreover, in Ref. [31] it is shown that adiabatic preparation can also be implemented efficiently on digital quantum computers, which also applies to our results. It is also important to design efficient physical realization of the proposed adiabatic path, which require engineering few-body Hamiltonians. Hamiltonian engineering can be realized in various platforms like the superconducting qubits [57], ion traps [58], and Rydberg atomic arrays [59], which potentially allows to realize large classes of Hamiltonians [60–62]. Finally, one can study the effect of noise on the adiabatic state preparation. In the presence of noise, we expect the adiabatic method provides an even bigger advantage over the sequential methods for preparing short-range correlated states, since more error accumulates during the sequential preparation (which takes a longer time).

Note added. During completion of this manuscript, we became aware of a related protocol that probabilistically creates the 1D and 2D AKLT states using const-depth circuits and postselection, with a success rate that exponentially decays with the system size N [63].

Acknowledgments. We thank Norbert Schuch and Yilun Yang for their insightful discussions. The research is part of the Munich Quantum Valley, which is supported by the Bavarian state government with funds from the Hightech Agenda Bayern Plus. We acknowledge funding from the German Federal Ministry of Education and Research (BMBF) through EQUAHUMO (Grant No. 13N16066) within the funding program Quantum Technologies—From Basic Research to Market, and the European Union’s Horizon 2020 research and innovation program under Grant No. 899354 (FET Open SuperQuLAN). The numerical calculations were performed using the ITensor Library [64].

- [1] M. Fannes, B. Nachtergaele, and R. F. Werner, Finitely correlated states on quantum spin chains, *Commun. Math. Phys.* **144**, 443 (1992).
- [2] D. Perez-García, F. Verstraete, M. M. Wolf, and J. I. Cirac, Matrix product state representations, *Quantum Info. Comput.* **7**, 401 (2007).
- [3] F. Verstraete and J. I. Cirac, Renormalization algorithms for quantum-many body systems in two and higher dimensions, [arXiv:cond-mat/0407066](https://arxiv.org/abs/cond-mat/0407066).
- [4] J. Eisert, M. Cramer, and M. B. Plenio, Colloquium: Area laws for the entanglement entropy, *Rev. Mod. Phys.* **82**, 277 (2010).
- [5] J. I. Cirac, D. Pérez-García, N. Schuch, and F. Verstraete, Matrix product states and projected entangled pair states: Concepts, symmetries, theorems, *Rev. Mod. Phys.* **93**, 045003 (2021).
- [6] H. J. Briegel and R. Raussendorf, Persistent Entanglement in Arrays of Interacting Particles, *Phys. Rev. Lett.* **86**, 910 (2001).
- [7] A. Y. Kitaev, Fault-tolerant quantum computation by anyons, *Ann. Phys.* **303**, 2 (2003).
- [8] D. M. Greenberger, M. A. Horne, and A. Zeilinger, Going beyond Bell's theorem, in *Bell's Theorem, Quantum Theory, and Conceptions of the Universe* (Springer, Berlin, 1989), p. 69.
- [9] W. Dür, G. Vidal, and J. I. Cirac, Three qubits can be entangled in two inequivalent ways, *Phys. Rev. A* **62**, 062314 (2000).
- [10] I. Affleck, T. Kennedy, E. H. Lieb, and H. Tasaki, Rigorous Results on Valence-Bond Ground States in Antiferromagnets, *Phys. Rev. Lett.* **59**, 799 (1987).
- [11] I. Affleck, T. Kennedy, E. H. Lieb, and H. Tasaki, Valence bond ground states in isotropic quantum antiferromagnets, *Commun. Math. Phys.* **115**, 477 (1988).
- [12] P. W. Anderson, The resonating valence bond state in La_2CuO_4 and superconductivity, *Science* **235**, 1196 (1987).
- [13] M. A. Levin and X.-G. Wen, String-net condensation: A physical mechanism for topological phases, *Phys. Rev. B* **71**, 045110 (2005).
- [14] H. J. Briegel, D. E. Browne, W. Dür, R. Raussendorf, and M. den Nest, Measurement-based quantum computation, *Nat. Phys.* **5**, 19 (2009).
- [15] M. Jarzyna and R. Demkowicz-Dobrzański, Matrix Product States for Quantum Metrology, *Phys. Rev. Lett.* **110**, 240405 (2013).
- [16] K. Azuma, K. Tamaki, and H. K. Lo, All-photonic quantum repeaters, *Nat. Commun.* **6**, 6787 (2015).
- [17] W. Huggins, P. Patil, B. Mitchell, K. Birgitta Whaley, and E. Miles Stoudenmire, Towards quantum machine learning with tensor networks, *Quantum Sci. Technol.* **4**, 024001 (2019).
- [18] C. Schön, E. Solano, F. Verstraete, J. I. Cirac, and M. M. Wolf, Sequential Generation of Entangled Multiqubit States, *Phys. Rev. Lett.* **95**, 110503 (2005).
- [19] N. Schuch, M. M. Wolf, F. Verstraete, and J. I. Cirac, Computational Complexity of Projected Entangled Pair States, *Phys. Rev. Lett.* **98**, 140506 (2007).
- [20] M. C. Bañuls, D. Pérez-García, M. M. Wolf, F. Verstraete, and J. I. Cirac, Sequentially generated states for the study of two-dimensional systems, *Phys. Rev. A* **77**, 052306 (2008).
- [21] H. Pichler, S. Choi, P. Zoller, and M. D. Lukin, Universal photonic quantum computation via time-delayed feedback, *Proc. Natl. Acad. Sci. USA* **114**, 11362 (2017).
- [22] M. P. Zaletel and F. Pollmann, Isometric Tensor Network States in Two Dimensions, *Phys. Rev. Lett.* **124**, 037201 (2020).
- [23] Z. Y. Wei, D. Malz, and J. I. Cirac, Sequential Generation of Projected Entangled-Pair States, *Phys. Rev. Lett.* **128**, 010607 (2022).
- [24] I. Schwartz, D. Cogan, E. R. Schmidgall, Y. Don, L. Gantz, O. Kenneth, N. H. Lindner, and D. Gershoni, Deterministic generation of a cluster state of entangled photons, *Science* **354**, 434 (2016).
- [25] J.-C. Besse *et al.*, Realizing a deterministic source of multipartite-entangled photonic qubits, *Nat. Commun.* **11**, 4877 (2020).
- [26] K. J. Satzinger *et al.*, Realizing topologically ordered states on a quantum processor, *Science* **374**, 1237 (2021).
- [27] A. Smith, B. Jobst, A. G. Green, and F. Pollmann, Crossing a topological phase transition with a quantum computer, *Phys. Rev. Res.* **4**, L022020 (2022).
- [28] T. Albash and D. A. Lidar, Adiabatic quantum computation, *Rev. Mod. Phys.* **90**, 015002 (2018).
- [29] M. Schwarz, K. Temme, and F. Verstraete, Preparing Projected Entangled Pair States on a Quantum Computer, *Phys. Rev. Lett.* **108**, 110502 (2012).
- [30] M. Schwarz, K. Temme, F. Verstraete, D. Perez-Garcia, and T. S. Cubitt, Preparing topological projected entangled pair states on a quantum computer, *Phys. Rev. A* **88**, 032321 (2013).
- [31] Y. Ge, A. Molnár, and J. I. Cirac, Rapid Adiabatic Preparation of Injective Projected Entangled Pair States and Gibbs States, *Phys. Rev. Lett.* **116**, 080503 (2016).
- [32] E. Cruz, F. Baccari, J. Tura, N. Schuch, and J. I. Cirac, Preparation and verification of tensor network states, *Phys. Rev. Res.* **4**, 023161 (2022).
- [33] See Supplemental Material at <http://link.aps.org/supplemental/10.1103/PhysRevResearch.5.L022037> for details on the adiabatic preparation of MPS and PEPS, as well as a study on the asymptotic power-law decay of the error density.
- [34] M. M. Wolf, G. Ortiz, F. Verstraete, and J. I. Cirac, Quantum Phase Transitions in Matrix Product Systems, *Phys. Rev. Lett.* **97**, 110403 (2006).
- [35] Note that an asymptotic scaling of this kind is not possible with the adiabatic ramps we use in this paper, as shown in Refs. [43,44,46] and the Appendix of Ref. [33].
- [36] A. Molnar, Y. Ge, N. Schuch, and J. I. Cirac, A generalization of the injectivity condition for projected entangled pair states, *J. Math. Phys.* **59**, 021902 (2018).
- [37] For all states we study in this paper, we simply set $\{Q_v\}$ on the boundary to be identity operators.
- [38] D. Perez-Garcia, F. Verstraete, M. M. Wolf, and J. I. Cirac, PEPS as unique ground states of local Hamiltonians, *Quantum Inf. Comput.* **8**, 650 (2008).
- [39] The Hamiltonian [Eq. (3)] can be efficiently constructed for arbitrary 1D MPS and 2D translationally invariant (TI) PEPS, which covers all examples studied in this paper. However, for a generic non-TI 2D PEPS, one cannot scalably obtain the few-site reduced density matrices $\{\rho_e\}$. In this case, it is possible to use a numerical optimization approach [65] to obtain a parent Hamiltonian with each term also only on a few sites.
- [40] One can transform $\{A_g\}$ to $\{A_{1/g}\}$ by first swapping the two indices in the auxiliary space (corresponding to transposing the matrices $\{A\}$), then swapping the physical indexes 2 and 3, and finally normalize the state.
- [41] The initial state $|\psi(0)\rangle$ can be prepared with local quantum circuit or adiabatic evolution of a constant depth (time).

- [42] We choose the interpolation functions such that they have a finite level of smoothness, which is both experimentally realistic and leads to an almost exponential decay of the error [cf. Eq. (8)] in a wide range of evolution time T . Since in we need to reach larger system size $N \approx 5000$ in 1D compared to $N \approx 100$ in 2D, we choose the function $s(t, T)_{1D}$ to be more smooth than $s(t, T)_{2D}$ at $t = 0$ and $t = T$.
- [43] G. Nenciu, Linear adiabatic theory. Exponential estimates, *Commun. Math. Phys.* **152**, 479 (1993).
- [44] G. A. Hagedorn and A. Joye, Elementary exponential error estimates for the adiabatic approximation, *J. Math. Anal. Appl.* **267**, 235 (2002).
- [45] D. A. Lidar, A. T. Rezakhani, and A. Hamma, Adiabatic approximation with exponential accuracy for many-body systems and quantum computation, *J. Math. Phys.* **50**, 102106 (2009).
- [46] A. T. Rezakhani, A. K. Pimachev, and D. A. Lidar, Accuracy versus run time in an adiabatic quantum search, *Phys. Rev. A* **82**, 052305 (2010).
- [47] Note that the sequential method prepares the state deterministically, while the adiabatic method always prepares the state approximately (with high fidelity), which is enough for practical purposes. Moreover, there could be a constant overhead to implement the Hamiltonian dynamics using quantum circuits, and this does not affect our statement that there will be a regime ($N \gg 1$) where the adiabatic preparation will be more efficient.
- [48] L. Zhou, S. Choi, and M. D. Lukin, Symmetry-protected dissipative preparation of matrix product states, *Phys. Rev. A* **104**, 032418 (2021).
- [49] R. Kaltenbaek, J. Lavoie, B. Zeng, S. D. Bartlett, and K. J. Resch, Optical one-way quantum computing with a simulated valence-bond solid, *Nat. Phys.* **6**, 850 (2010).
- [50] M. Lemm, A. W. Sandvik, and L. Wang, Existence of a Spectral Gap in the Affleck-Kennedy-Lieb-Tasaki Model on the Hexagonal Lattice, *Phys. Rev. Lett.* **124**, 177204 (2020).
- [51] N. Pomata and T. C. Wei, Demonstrating the Affleck-Kennedy-Lieb-Tasaki Spectral Gap on 2D Degree-3 Lattices, *Phys. Rev. Lett.* **124**, 177203 (2020).
- [52] M. Koch-Janusz, D. I. Khomskii, and E. Sela, Affleck-Kennedy-Lieb-Tasaki State on a Honeycomb Lattice from t_{2g} Orbitals, *Phys. Rev. Lett.* **114**, 247204 (2015).
- [53] The 2D AKLT state studied here requires to block six sites in a hexagon [cf. Fig. 1(c)] to make the tensor injective.
- [54] M. Lubasch, J. I. Cirac, and M.-C. Bañuls, Algorithms for finite projected entangled pair states, *Phys. Rev. B* **90**, 064425 (2014).
- [55] This is also true for the path in Refs. [31,32]. However, the large support of each Hamiltonian term makes it still difficult to simulate the adiabatic dynamics along that path.
- [56] M. J. Kastoryano and A. Lucia, Divide and conquer method for proving gaps of frustration-free Hamiltonians, *J. Stat. Mech.: Theory Exp.* (2018) 033105.
- [57] A. Mezzacapo, L. Lamata, S. Filipp, and E. Solano, Many-Body Interactions with Tunable-Coupling Transmon Qubits, *Phys. Rev. Lett.* **113**, 050501 (2014).
- [58] A. Bermudez, D. Porras, and M. A. Martin-Delgado, Competing many-body interactions in systems of trapped ions, *Phys. Rev. A* **79**, 060303(R) (2009).
- [59] P. Scholl *et al.*, Microwave engineering of programmable XXZ Hamiltonians in arrays of Rydberg atoms, *PRX Quantum* **3**, 020303 (2022).
- [60] T. Cubitt, A. Montanaro, and S. Piddock, Universal quantum Hamiltonians, *Proc. Natl. Acad. Sci.* **115**, 9497 (2018).
- [61] L. Zhou and D. Aharonov, Strongly universal Hamiltonian simulators, [arXiv:2102.02991](https://arxiv.org/abs/2102.02991).
- [62] J. Choi, H. Zhou, H. S. Knowles, R. Landig, S. Choi, and M. D. Lukin, Robust Dynamic Hamiltonian Engineering of Many-Body Spin Systems, *Phys. Rev. X* **10**, 031002 (2020).
- [63] B. Murta, P. M. Q. Cruz, and J. Fernández-Rossier, Preparing valence-bond-solid states on noisy intermediate-scale quantum computers, *Phys. Rev. Res.* **5**, 013190 (2023).
- [64] M. Fishman, S. R. White, and E. M. Stoudenmire, The ITensor software library for tensor network calculations, *SciPost Phys. Codebases* **4**, (2022).
- [65] G. Giudici, J. I. Cirac, and N. Schuch, Locality optimization for parent Hamiltonians of tensor networks, *Phys. Rev. B* **106**, 035109 (2022).